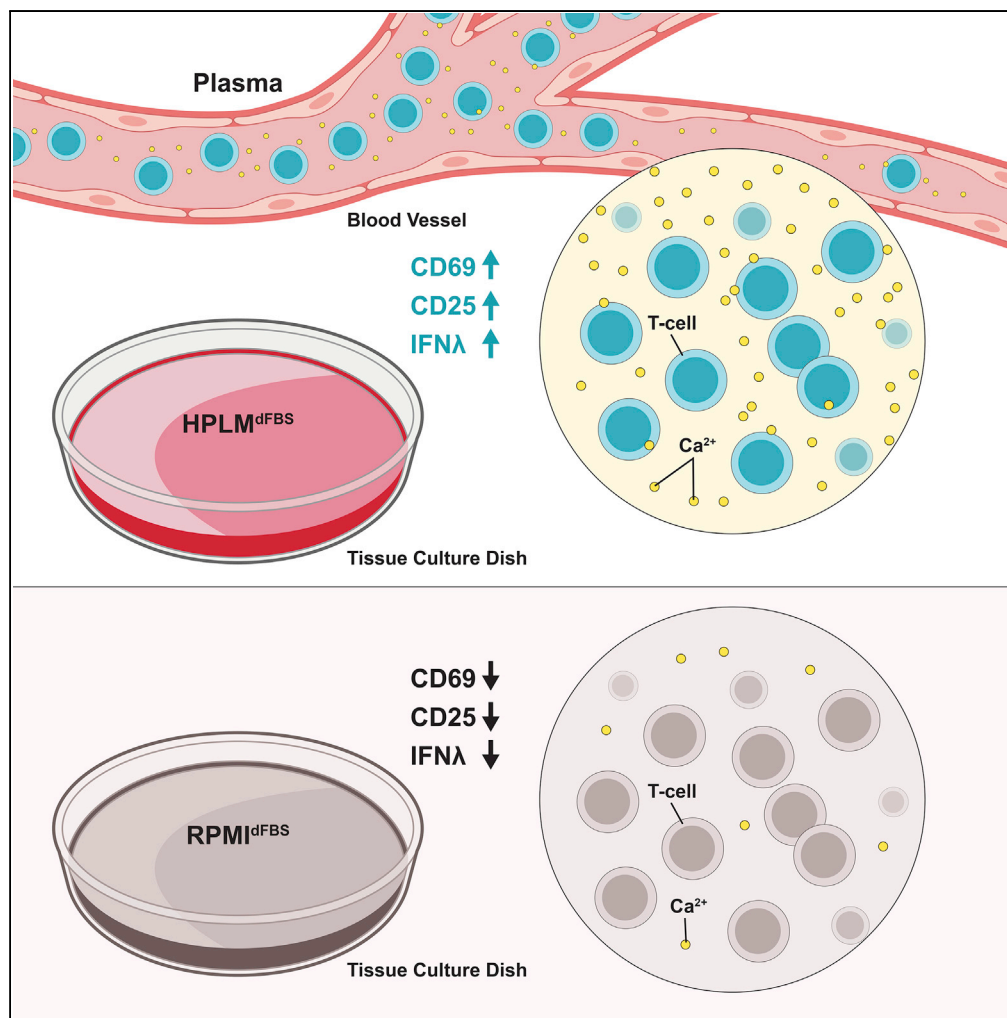


Article

Human Plasma-like Medium Improves T Lymphocyte Activation



Michael A. Leney-Greene, Arun K. Boddapati, Helen C. Su, Jason R. Cantor, Michael J. Lenardo

michael.lenardo@nih.gov

HIGHLIGHTS

Activation of T lymphocytes in plasma-like medium is much more efficient

RPMI is severely hypocalcemic relative to human plasma and this impacts activation

Non-physiological levels of nutrients in RPMI alter lymphocyte metabolism

Leney-Greene et al., iScience
23, 100759
January 24, 2020
<https://doi.org/10.1016/j.isci.2019.100759>



Article

Human Plasma-like Medium Improves T Lymphocyte Activation

Michael A. Leney-Greene,^{1,2,7} Arun K. Boddapati,^{3,4} Helen C. Su,^{2,5} Jason R. Cantor,^{6,7,8,9,10} and Michael J. Lenardo^{1,2,10,11,*}

SUMMARY

T lymphocytes are critical for effective immunity, and the ability to study their behavior *in vitro* can facilitate major insights into their development, function, and fate. However, the composition of human plasma differs from conventional media, and we hypothesized that such differences could impact immune cell physiology. Here, we showed that relative to the medium typically used to culture lymphocytes (RPMI), a physiologic medium (human plasma-like medium; HPLM) induced markedly different transcriptional responses in human primary T cells and in addition, improved their activation upon antigen stimulation. We found that this medium-dependent effect on T cell activation is linked to Ca²⁺, which is six-fold higher in HPLM than in RPMI. Thus, a medium that more closely resembles human plasma has striking effects on T cell biology, further demonstrates that medium composition can profoundly affect experimental results, and broadly suggests that physiologic media may offer a valuable way to study cultured immune cells.

INTRODUCTION

Adaptive immune systems involve the movement of immune cells throughout the internal milieu of the blood and interstitial spaces to recognize foreign agents and respond to ensure the health of the host. T lymphocytes are central effectors of immunity in infectious diseases, autoimmunity, and cancer. T cell activation by cognate antigen is a complex process influenced by both intrinsic and extrinsic factors. Ligation of the $\alpha\beta$ -T cell receptor by peptide antigens bound to major histocompatibility complex (MHC) class I/II initiates a number of signaling events culminating in the activation of a robust transcriptional program, which is key for an appropriate response.

The extracellular environment of the T lymphocyte has increasingly been recognized as a major influence on the characteristics and magnitude of the immune response. Namely, the availability of nutrients/second messengers in the environment, and the consequent changes in the metabolic status of the cell, are critical for shaping an appropriate T cell response. Recent publications have highlighted the influence of lipids, glucose, and amino acid metabolism on both the magnitude and characteristics of T cell responses (Pearce et al., 2009; van der Windt and Pearce, 2012; Sinclair et al., 2013; O'Sullivan et al., 2014; Buck et al., 2017; Ma et al., 2017; Werner et al., 2017; Jacobs et al., 2018). In addition to metabolic changes, ligation of the T cell receptor also induces the influx of extracellular calcium ions via the STIM/Orai channel, leading to activation of downstream transcription factors such as NFAT (Smith-garvin et al., 2010; Derler et al., 2016). Although a complete deficiency of this process has been studied in multiple contexts, the influence of subtler variations in extracellular calcium levels on T cell activation remain unclear (Feske et al., 2006; Prakriya et al., 2006).

Formulations of common cell culture media such as RPMI-1640 were developed in the mid-20th century to optimize *in vitro* growth of cell lines and have since undergone remarkably little change (Eagle, 1955; McCoy et al., 1959; Moore et al., 1966). Despite a growing focus on the effects of metabolic changes during T cell activation and proliferation, culture conditions that more closely resemble the *in vivo* milieu have not been studied. Recently, several studies in non-immune cells have described the use of modified traditional media or new systematically constructed synthetic media designed to either improve growth in cell culture or to better model the *in vivo* environment (Favaro et al., 2012; Schug et al., 2015; Pan et al., 2016; Cantor et al., 2017; Vande Voorde et al., 2019). Among these is human plasma-like medium (HPLM), which contains a cocktail of 31 components that are absent from the defined formulations of RPMI and other commonly used basal culture media (Cantor et al., 2017). HPLM further contains at physiologically relevant concentrations other typical media components such as glucose, amino acids, and salt ions. It is worth noting that all

¹Molecular Development of the Immune System Section, Laboratory of Immune System Biology, National Institute of Allergy and Infectious Diseases, National Institutes of Health, Bethesda, MD 20892, USA

²Immunology Graduate Group, Biomedical Graduate Studies, University of Pennsylvania, Philadelphia, PA 19104, USA

³NIAID Collaborative Bioinformatics Resource (NCBR), National Institute of Allergy and Infectious Diseases, National Institutes of Health, Bethesda, MD, USA

⁴Advanced Biomedical Computational Science, Frederick National Laboratory for Cancer Research, Frederick, MD, USA

⁵Human Immunological Diseases Section, Laboratory of Clinical Immunology and Microbiology, National Institute of Allergy and Infectious Diseases, National Institutes of Health, Bethesda, MD 20892, USA

⁶Morgridge Institute for Research, 330 North Orchard Street, Madison, WI 53715, USA

⁷Department of Biochemistry, University of Wisconsin-Madison, Madison, WI 53706, USA

⁸Department of Biomedical Engineering, University of Wisconsin-Madison, Madison, WI 53706, USA

⁹Carbone Cancer Center, University of Wisconsin-Madison, 600 Highland Avenue, Madison, WI 53705, USA

¹⁰These authors contributed equally

¹¹Lead Contact

*Correspondence:

michael.lenardo@nih.gov

<https://doi.org/10.1016/j.isci.2019.100759>



of these defined components may be otherwise present at non-physiological levels in fetal bovine serum (FBS), the most widely used tissue culture supplement (Cantor et al., 2017). And therefore, HPLM is instead supplemented with 10% dialyzed FBS (HPLM^{dFBS}). Here, we asked how HPLM^{dFBS} influences gene expression and activation of cultured primary human T lymphocytes.

RESULTS

Transcriptome Analysis Reveals Extensive Differences in T Lymphocytes Activated in HPLM^{dFBS} Compared with RPMI^{dFBS}

T lymphocytes *in vivo* undergo broad transcriptional re-programming following TCR activation, and this process occurs in the context of a rich internal milieu containing high levels of amino acids, lipids, and a variety of small organic metabolites (Crabtree, 1989). In contrast, typical *in vitro* methods used to study these same processes are based on T cells cultured in RPMI, which contains a collection of nutrients at non-physiologic concentrations (Moore et al., 1967). Therefore, we evaluated activation in naive CD4/CD8⁺ T cells stimulated in HPLM^{dFBS} compared with RPMI analogously supplemented with 10% dialyzed serum (RPMI^{dFBS}) to restrict our downstream analysis of potential phenotypic differences to defined media components only (Figure 1A, Table S1). We then activated purified human naive T lymphocytes from three individual donors with plate-bound anti-CD3/CD28 antibodies for 48 or 120 h in either HPLM^{dFBS} or RPMI^{dFBS}, isolated polyadenylated mRNAs, and characterized the transcriptional differences between these two conditions via deep sequencing. Principal component analysis revealed changes between 48 and 120 h of activation independently of the medium used. Nonetheless, the 2nd and 3rd principal components divided each group of samples (RPMI^{dFBS}-48 h, RPMI^{dFBS}-120 h, HPLM^{dFBS}-48 h, and HPLM^{dFBS}-120 h) into clear clusters revealing the transcriptional differences between HPLM^{dFBS} and RPMI^{dFBS} (Figure 1C). We next used gene set enrichment analysis (GSEA) to identify statistically significant differences in 29 different Kyoto encyclopedia of genes and genomes (KEGG) pathways (Kanehisa and Goto, 2000; Kanehisa et al., 2019). Nine pathways were significantly different at 48 h, 19 significantly different at 120 h, and one pathway was shared between both timepoints (Figure S1). Among these we observed a striking enrichment of pathways involved in DNA replication and cell cycle in HPLM^{dFBS} at 120 h post-activation and an enrichment of pathways involved in T cell activation at 48 h (Figure S1). In particular, essentially every gene in the KEGG DNA replication pathway exhibited increased expression in HPLM^{dFBS} relative to RPMI^{dFBS} (Figure 1D). Thus, T cell activation in HPLM^{dFBS} was superior to RPMI^{dFBS}, and this difference was readily apparent as early as 48 h post activation.

There were also marked medium-dependent transcriptional differences across several metabolic pathways (Table 1). For instance, we found that HPLM^{dFBS} induced large increases in the expression of genes involved in amino acid metabolism, including the KEGG annotated pathways: arginine/proline metabolism; glycine/threonine/serine metabolism; and alanine, aspartate, and glutamate metabolism. These differences may be driven as a result of the roughly 2–10 fold differences in availability of arginine, aspartate, serine, and glutamate between the two media (Table S1). We also found that HPLM^{dFBS} induced increased relative expression of genes involved in the p53 signaling pathway as well as in various nucleic acid metabolism pathways (e.g. DNA repair, pyrimidine metabolism, RNA polymerase, spliceosome, and homologous recombination). In contrast, HPLM^{dFBS} also induced a relative decrease in the expression of genes associated with several other pathways, including glycerophospholipid and cytochrome p450 metabolism, cell adhesion, allograft rejection, graft vs. host disease, type 1 diabetes, cytokine receptor interactions, and autoimmune thyroid disease. Taken together, these results suggest that HPLM^{dFBS} promotes a T cell expression signature that is more to promote proliferation and to restrain autoimmunity.

HPLM^{dFBS} Is Superior to RPMI^{dFBS} in Supporting Naive Human CD4/CD8⁺ T Cell Activation

Guided by our RNA-Seq data, we hypothesized that T cell activation and proliferation would be more efficient in HPLM^{dFBS}. Thus, we went on to measure markers of activation in antigen-stimulated naive human T cells (Figure 1). In both CD4⁺ and CD8⁺ T cells from five different healthy donors, we observed a significant increase in CD25 and CD69 in HPLM^{dFBS} compared with RPMI^{dFBS} (Figure 2A). We also carried out time courses spanning multiple days and the differences in this case were robust at every time point examined (Figure S2A). In addition, the use of increased anti-CD3/CD28 antibody concentrations during the activation led to a nearly equivalent maximal response rate in both conditions (i.e. >90% positive for both CD25 and CD69) (Figure 2A). This result suggests that HPLM^{dFBS} effectively reduces the activation threshold, as further supported both by the relatively unique appearance of large activated T cell clusters in the HPLM^{dFBS} cultures, as well as a marked difference in cell size between the two conditions (Figure 2B). Given

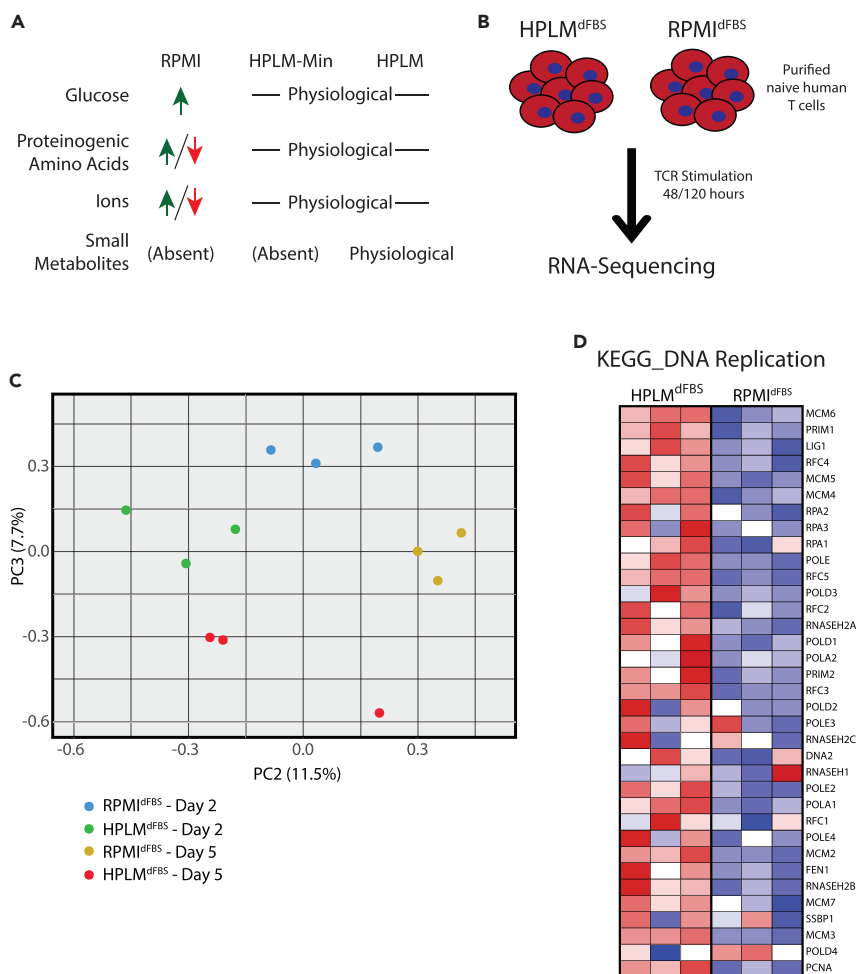


Figure 1. Transcriptomic Analysis Reveals Major Differences between Human Lymphocytes Activated in HPLM^{dFBS} Relative to RPMI^{dFBS}

(A) Schematic of the comparative compositions of RPMI^{dFBS}, HPLM^{dFBS}, and HPLM^{dFBS}-Min. Detailed composition can be found in Table S1.

(B) Experimental outline for T cell activation in either HPLM^{dFBS} or RPMI^{dFBS} and downstream transcriptome analysis.

(C) Transcriptional differences between primary naïve human mixed CD4⁺ and CD8⁺ T cells from three different donors activated in HPLM^{dFBS} or RPMI^{dFBS} as depicted in (B) were measured via RNA-sequencing. These data were used to generate PCA plots showing principal components 2 and 3 at the indicated timepoints.

(D) Heatmap showing the Log₂(fold change) in transcript abundance for genes involved in the KEGG DNA replication pathway using the RNA-sequencing data generated as described in (B).

that the T cells activated in RPMI^{dFBS} exhibited both a bimodal size distribution and much larger absolute size within the unstimulated population, this relative cell size difference was likely driven by defective activation. Furthermore, as anticipated from the transcriptional differences described earlier, we also found that the rapid proliferation of activated T cells in HPLM^{dFBS} was far less apparent in RPMI^{dFBS} (Figure 2C). Lastly, although HPLM was not designed to mimic the *in vivo* milieu of mice, we also tested activation of murine T cells in HPLM^{dFBS} versus RPMI^{dFBS}, as this is a popular model used in the field. Again, we observed greatly improved activation in HPLM^{dFBS}, suggesting that the mechanism responsible is evolutionarily conserved. In addition, these results would suggest that HPLM is better suited to the *in vitro* culture of both murine and human T cells.

Physiological Calcium Availability Augments T Cell Activation

We next asked which component(s) of HPLM^{dFBS} dictated the relative differences in T cell activation. To do so, we first compared T cell activation HPLM^{dFBS}, HPLM-Min (which contains only the defined amino acids,

	Fold Change in Expression in HPLM ^{dFBS}
Serine Biosynthesis	
PHGDH	6.10
PSAT1	5.30
PSPH	1.25
Glycine, Arginine, Proline Biosynthesis	
SHMT1	1.80
SHMT2	1.33
PYCR1	4.32
ASS1	81.00
Aspartate Biosynthesis	
GOT1	1.45
Cholesterol Biosynthesis	
HMGCS1	0.38
HMGCR	0.49
MVD	0.48
FDFT1	0.47

Table 1. Transcriptional Differences in Metabolic Genes in T Cells Cultured in HPLM^{dFBS}

glucose, vitamins, salts, and 10% dialyzed serum; see Table S1), and (Cantor et al., 2017) and RPMI^{dFBS} (Figure 1A, Table S1). Further, we also included a medium derivative in which we supplemented all HPLM-specific polar metabolites to RPMI^{dFBS} (RPMI-Metabolites). We ultimately observed an equivalent extent of activation in the HPLM^{dFBS} and HPLM-Min conditions and a significantly reduced relative extent of activation in both RPMI^{dFBS} and RPMI-metabolites (Figure 3A). These results suggest that in this context, the relative differences in activation between HPLM^{dFBS} and RPMI^{dFBS} were instead due to concentration differences in amino acids, glucose, or salt ions. And indeed, one striking concentration difference among these is that of calcium (Ca²⁺), which is provided by HPLM at a defined concentration of 2.4 mM but is instead present in RPMI at a defined level of 0.4 mM, (Table S1), which is markedly hypocalcemic relative to the *in vivo* milieu (2–2.5 mM) (Goldstein, 1990). In turn, we in fact found that supplementing RPMI^{dFBS} with 2 mM CaCl₂ (RPMI+Ca²⁺) was sufficient to achieve T cell activation to an extent equivalent to that seen in HPLM^{dFBS} (Figure 3A).

It is worth noting that basal media used to culture T lymphocytes (often RPMI) are instead typically supplemented with 10% unmodified FBS (RPMI^{FBS}), and so we next wanted to determine the Ca²⁺ concentration of RPMI^{FBS} and ask how this particular complete medium influenced relative T lymphocyte activation as well. We found that [Ca²⁺] was approximately 3.9 mM in our typical stock FBS, and thus, a 10% supplement to basal RPMI would result in a RPMI^{FBS} Ca²⁺ concentration of ~0.8 mM, a value that is still considered hypocalcemic although is closer to physiologic levels. We next found that TCR stimulation of naive T cells in RPMI^{FBS} induced activation to an extent nearly equivalent to that in HPLM^{dFBS} (Figure 3B), suggesting that 10% unmodified FBS provides RPMI sufficient Ca²⁺ to achieve comparable activation. We next examined Ca²⁺ flux following TCR stimulation in RPMI^{dFBS}, RPMI^{Ca2+}, and HPLM^{dFBS}. It is worth noting that most calcium flux protocols are carried out in Hank's balanced salt solution or Ringer's solution; however, some studies have described a decreased Ca²⁺ flux in RPMI relative to these solutions (Prakriya et al., 2006; Gwack et al., 2008; Bertin et al., 2014). We observed a striking decrease in the amount of Ca²⁺ entering T cells following activation in RPMI^{dFBS}, as compared with either HPLM^{dFBS} or RPMI^{Ca2+} (Figure 3C). Taken together, our results suggest that the relatively greater threshold for T cell activation in RPMI^{dFBS} resulted from lower Ca²⁺ availability.

Our results also raise the possibility that *in vivo* Ca²⁺ levels can influence T cell activation and that hypocalcemic (or hypercalcemic) patients may be more prone to immunodeficiency (or autoimmunity), and in fact

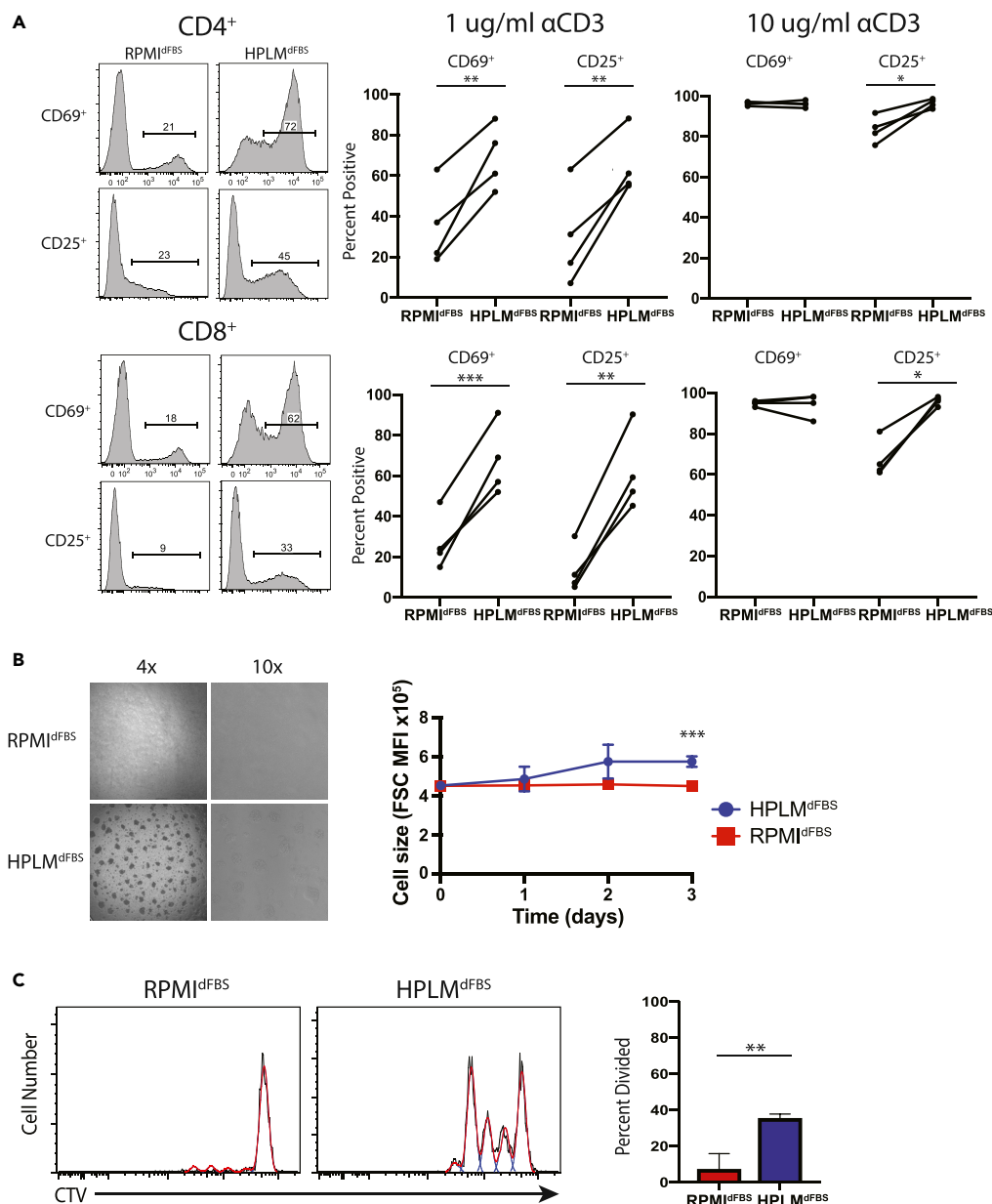


Figure 2. Primary Human T Cell Activation Is Superior in HPLM^{dFBS} Compared with RPMI^{dFBS}

(A) Flow cytometric measurement of T cell activation markers CD25 and CD69 on purified naive human T cells following stimulation with either 1 or 10 μg of plate-bound anti-CD3 (αCD3)/CD28 in HPLM^{dFBS} or RPMI^{dFBS} for 16 h. Data shown are representative of four different experiments each conducted with cells isolated from a different healthy donor (Student's t test; paired; two-tails; *p < 0.05, **p < 0.01, ***p < 0.001).

(B) Bright-field microscopy images of naive T cells stimulated with 1 μg of plate-bound anti-CD3/CD28 in either HPLM^{dFBS} or RPMI for 16 h.

(C) Flow cytometry histograms of CellTrace Violet staining of naive T cells stimulated in either HPLM^{dFBS} or RPMI^{dFBS} (left) with quantitation of the fraction of CD4⁺ T cells that have undergone at least one division (right). Columns represent the mean of three experiments, each done with cells isolated from a different healthy donor (Student's t test; unpaired; two-tails; *p < 0.05). Error bars represent the SEM.

others had previously shown that extracellular [Ca²⁺] can influence cytokine production in murine T cells (Zimmermann et al., 2015). Moreover, our observations indicated that RPMI^{dFBS} poorly recapitulates *in vivo* conditions, given the hypocalcemic conditions it provides to cells. Thus, we next titrated Ca²⁺ levels in basal RPMI in 0.5 mM increments, up to a maximum of 2.2 mM, and then measured TCR-induced Ca²⁺

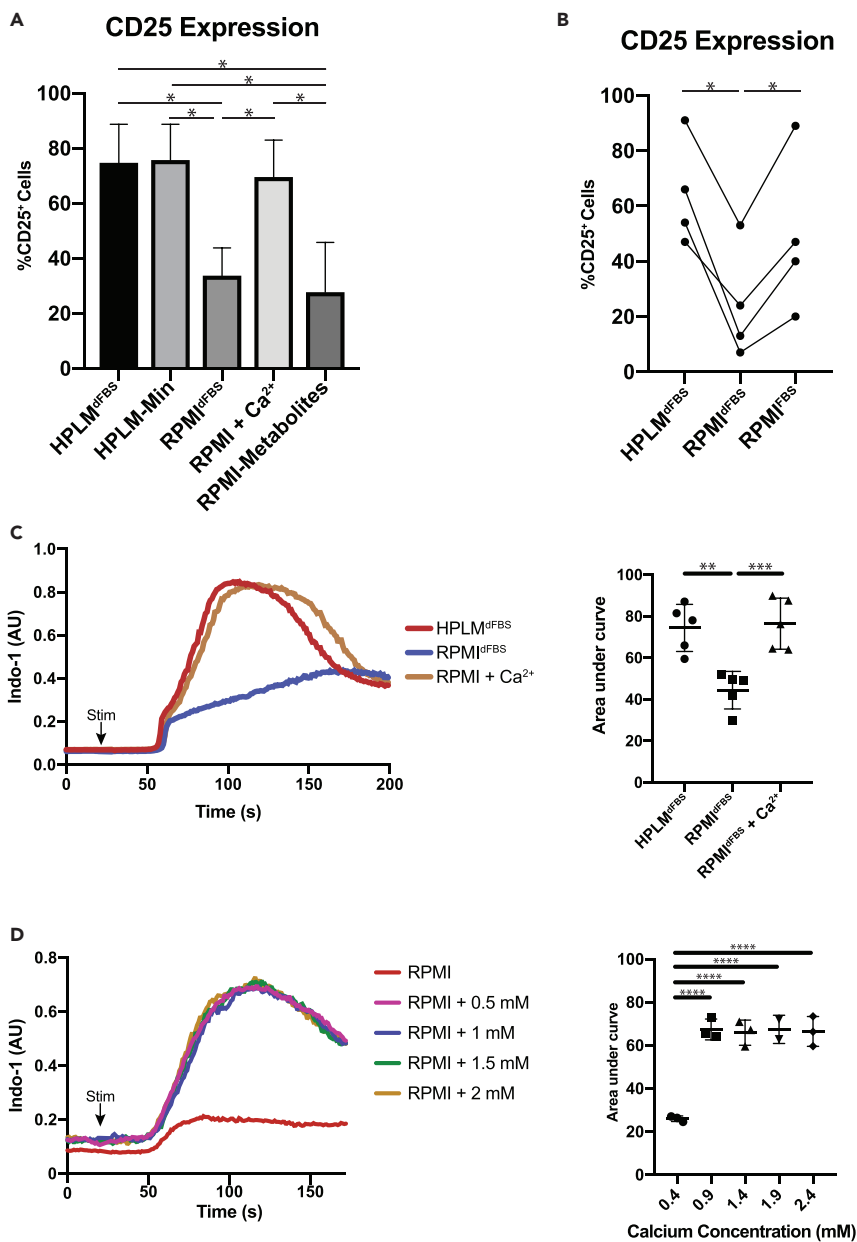


Figure 3. RPMI^{dFBS} Is Severely Hypocalcemic Relative to Human Plasma and HPLM^{dFBS}

(A) Measurement of activation marker CD25 on CD4⁺ T cells comparing RPMI^{dFBS} and HPLM^{dFBS}-min supplemented with various metabolite components unique to HPLM^{dFBS}. Columns represent the mean with error bars showing the standard error (one-way ANOVA comparing other conditions to HPLM^{dFBS} with p values calculated by Dunnett test; *p < 0.05).

(B) Measurement of activation marker CD25 on CD4⁺ T cells activated in HPLM^{dFBS}, RPMI^{dFBS}, or RPMI^{FBS}. Experiment was repeated four times with each repeat using a different healthy human donor (one-way ANOVA; Tukey's test; *p < 0.05).

(C) Flow cytometric plots of calcium flux following primary stimulation of isolated human CD8⁺ T lymphocytes in either RPMI^{dFBS} or HPLM^{dFBS} (left) as well as quantification of the area under the curve (right). Quantification shows data from five experiments each done with a different individual donor, and error bars show standard error (one-way ANOVA; Tukey's test; **p < 0.01, ***p < 0.001).

(D) Flow cytometric plots of calcium flux following primary stimulation of isolated human CD8⁺ T lymphocytes in RPMI^{dFBS} supplemented with the indicated concentrations of calcium chloride. Quantification shows data from five experiments each done with a different individual donor, and error bars show standard error (one-way ANOVA; Tukey's test; **p < 0.01, ***p < 0.001).

flux. We again observed that basal RPMI induced a meager Ca^{2+} flux, but the supplementation of $[\text{Ca}^{2+}]$ from 0.7 to 2.2 mM yielded Ca^{2+} fluxes that were virtually identical in both magnitude and kinetics (Figure 3D), suggesting that even at the lower end of physiologically reported levels, the Ca^{2+} flux rates can reach achieve maximum levels and that greater Ca^{2+} levels likely do not affect the propensity of *in vivo* T cell activation. Nonetheless, the $[\text{Ca}^{2+}]$ in basal RPMI is insufficient to promote full Ca^{2+} flux or T cell activation.

HPLM^{dFBS} Promotes CD8⁺ T Cell Effector Cytokine Production

We next evaluated cytokine production in CD8⁺ T cells activated in HPLM^{dFBS} or HPLM^{dFBS}-Min. We activated T cells in RPMI^{dFBS} and grew them for 14 to 21 days supplemented with IL-2 prior to restimulation and measurement of cytokine production. We find that TNF α and IFN γ production was similar in HPLM^{dFBS} or HPLM^{dFBS}-Min but substantially greater than RPMI^{dFBS} (Figure 4A). Similar results were obtained with phorbol myristate acetate (PMA) and ionomycin or anti-CD3 antibodies cross-linked with protein A. IFN γ production was slightly reduced in HPLM^{dFBS} compared with HPLM^{dFBS}-min although this did not reach statistical significance. We next examined whether this difference was due to the media composition during the initial stimulation or the subsequent restimulation by activating and expanding the cells in HPLM^{dFBS} or RPMI^{dFBS} and then switching them to other media just prior to restimulation (Figure 4B). Under these conditions, we observed robust cytokine production in cells that were activated in HPLM^{dFBS} or RPMI^{dFBS} and then transferred to HPLM^{dFBS} or RPMI^{dFBS} supplemented with 2mM Ca^{2+} (Figure 4B). However, irrespective of the initial activation medium, cells instead transferred to RPMI^{dFBS} exhibited reduced cytokine production levels, suggesting that $[\text{Ca}^{2+}]$ is a critical factor at the time of restimulation.

CD19 CAR-T Cell Transduction Efficiency in HPLM^{dFBS} Is Similar to Other Commonly Used Media

T lymphocytes have become a central focus in the cancer immunotherapy field, and many clinical protocols require *in vitro* culture and expansion of human T cells engineered with chimeric antigen receptors (CAR-T cell) (Newick et al., 2018). Therefore, we wanted to ask whether pan naive T cells cultured in HPLM^{dFBS} exhibit improved transduction efficiency for lentiviruses that express CAR-T cell receptors. To do so, we first evaluated how HPLM^{dFBS} affected activation relative to that in two other synthetic media commonly used in clinical CAR-T expansion protocols: a mixture of AIM V and RPMI (supplemented with 5% human serum, referred to as AIM V here) and X-VIVO 15 (serum free). Following stimulation with plate bound anti-CD3/CD28 antibodies, we observed equivalent CD25 expression levels in HPLM^{dFBS}, HPLM^{dFBS}-Min, and AIM V, which were ultimately greater than those induced by culture in X-VIVO 15 (Figure 5A). We then observed that the lentiviral transduction efficiencies of both CD4⁺ and CD8⁺ T cells were equivalent in HPLM^{dFBS}, HPLM^{dFBS}-Min, and AIM V media and greater than those in X-VIVO 15 (Figure 5B). Taken together, HPLM^{dFBS} performs comparably or better than commonly used culture media that have been used to generate CAR-expressing T cells.

DISCUSSION

The development of cell culture techniques in the mid 20th century heralded an enormous advance in life sciences research by permitting tissue-free *in vitro* studies of cell physiology. However, media formulations developed in the 1960s remain almost universally used today. Here, we took advantage of a recent effort to systematically develop a new cell culture medium that was designed to more closely model human plasma (HPLM) by extending the use of HPLM to the study of primary human lymphocytes. We show that compared to RPMI^{dFBS}, HPLM^{dFBS} induces a much more robust activation of naive T cells and a marked increase in the secretion of effector cytokines. Further, comparative RNA-Seq methods revealed a large number of medium-dependent T cell transcriptional differences across several metabolic pathways.

Through the use of HPLM, we also find that calcium is a rate-limiting component for lymphocyte activation, a result that corroborates recent work that describes the induction of acute Ca^{2+} flux following TCR engagement (Zhang et al., 2005; Prakriya et al., 2006). Others have also described a relative increase in effector cytokine secretion for murine T cells cultured in IMDM ($[\text{Ca}^{2+}] = 1.5$ mM) or calcium supplemented-RPMI^{dFBS} compared with basal RPMI (Zimmermann et al., 2015). Similarly, we found in primary human T cells that relative activation, proliferation, and effector cytokine secretion are reduced in RPMI^{dFBS} lacking any additional Ca^{2+} supplementation. It is likely that the use of 10% FBS as a common supplement to basal media sufficiently augments the defined calcium concentration of RPMI, as we measured the Ca^{2+}

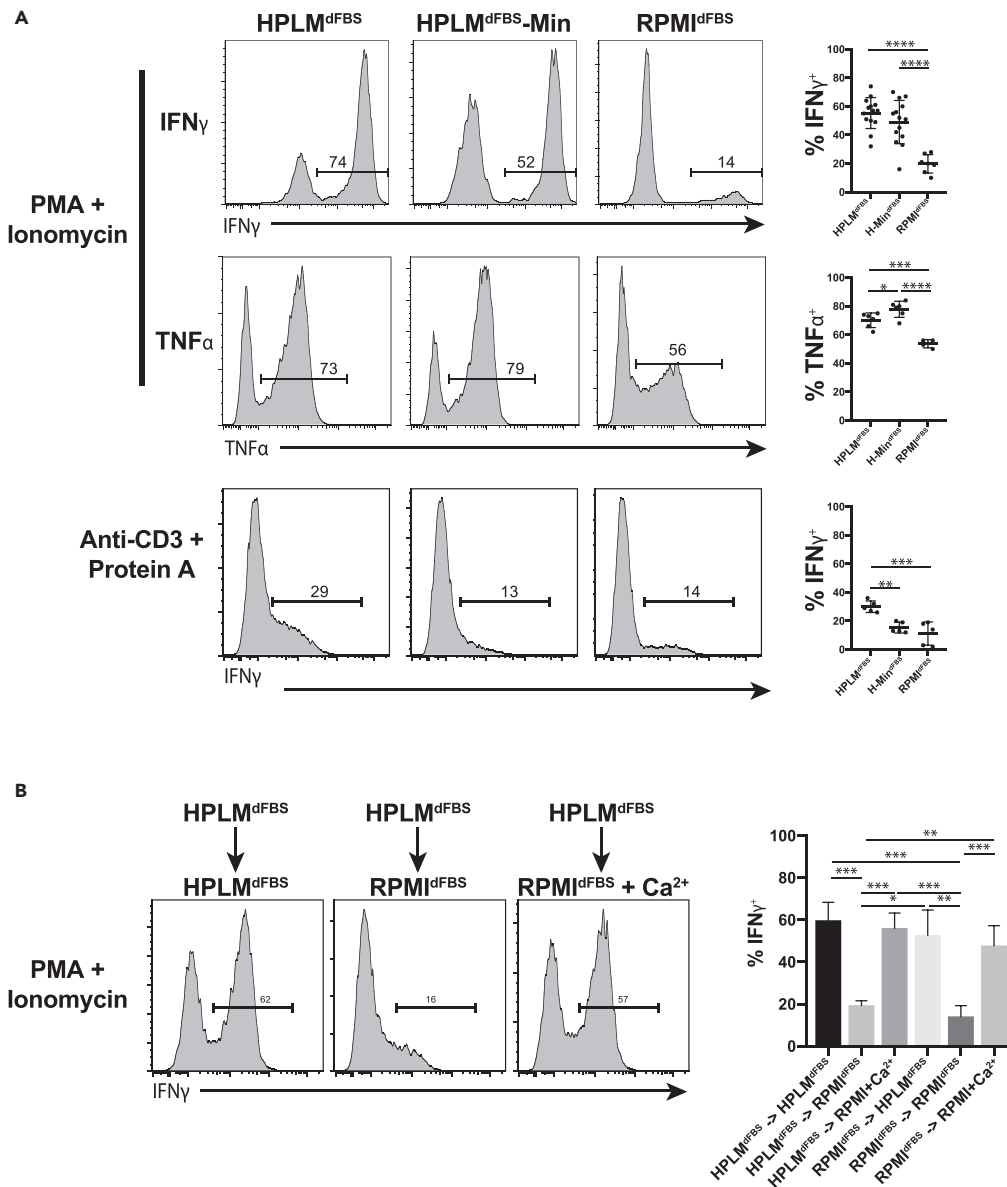


Figure 4. T Cells Activated in HPLM^{dFBS} Produce Higher Levels of Effector Cytokines

(A) Levels of cytokines produced in primary human T lymphocytes following restimulation after being expanded in the indicated medium. T lymphocytes from 5 to 14 individuals were tested across two to three experiments, with the error bars representing standard deviation (one-way ANOVA; Tukey's test; *p < 0.05, **p < 0.01, ***p < 0.001, ****p < 0.0001).

(B) Quantification of cytokine production in primary human T lymphocytes expanded in the indicated medium, switched to fresh medium of the indicated type, and then restimulated. Columns represent the mean of measurements from three experiments each with two individuals, with the error bars representing the standard error (one-way ANOVA; Tukey's test; *p < 0.05, **p < 0.01, ***p < 0.001).

levels of stock FBS as approximately 3.9 mM. Although our current study suggests that the resultant RPMI^{FBS} Ca²⁺ concentration (~0.8 mM), which still corresponds to a severely hypocalcemic condition, is sufficient to achieve maximal TCR-induced Ca²⁺ flux and activation, it is now clear that calcium level is an independent parameter that should be considered in studies of T cell biology. For instance, it is possible that the cross-linking of anti-CD3 antibodies used in the calcium flux methods masks an underlying defect that would be present in response to physiological antigens. Further, the calcium flux assay only assesses calcium changes for the first several minutes of a response, whereas the activation process is much more dynamic and can extend over the course of h/day *in vivo*.

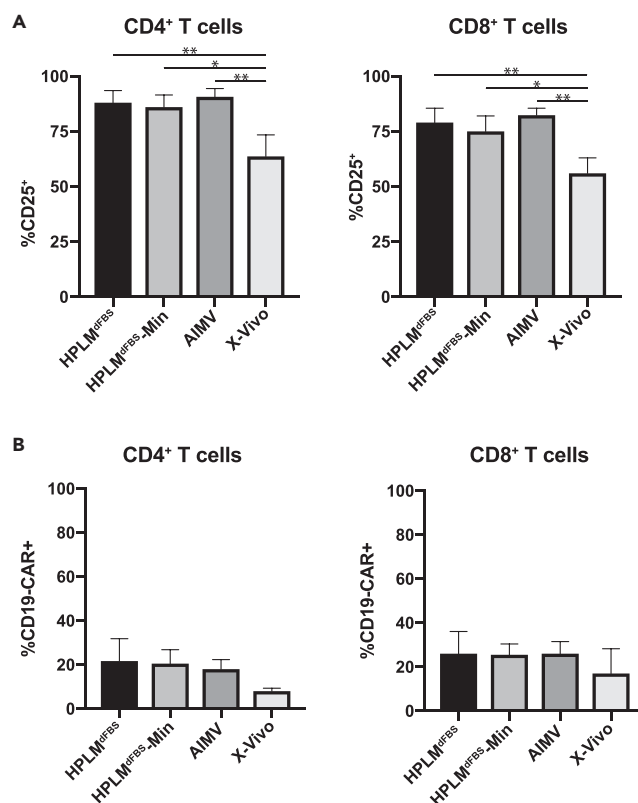


Figure 5. Lentiviral Transduction Rates Are Equivalent in T Cells Cultured in HPLM^{dFBS} and Conventional Culture Media

(A) Quantification of levels of activation markers in CD4⁺ (left panel) and CD8⁺ T cells following activation in the indicated medium. Columns represent the mean of measurements from three experiments each conducted with cells from a different individual, with error bars representing the standard error (one-way ANOVA; Tukey's test; *p < 0.05, **p < 0.01). (B) Quantification of transduction efficiency human CD4⁺ (left panel) and CD8⁺ T cells (right panel) with CD19-CAR expressing lentiviruses activated in the indicated media. Columns represent the mean of measurements from three experiments each conducted with cells from a different individual, with error bars representing the standard error (one-way ANOVA; Tukey's test).

Although our results comparing HPLM^{dFBS} with a derivative containing only amino acids, glucose, vitamins, salts, and 10% dialyzed serum (HPLM-min) did not suggest an induction of dramatically different phenotypic outputs, a caveat of our study is that prior work with HPLM^{dFBS} described a much more robust serum dialysis procedure (Cantor et al., 2017). Thus, it is possible that our commercial source of this supplement was far less stringently dialyzed, and in turn, perhaps still contained appreciable levels of several polar metabolites, which would mask any putative differences between the two HPLM derivatives.

This study was primarily focused on the impact of the extracellular milieu on early T cell activation events. As we observed significant differences in the activation efficiency of human T lymphocytes cultured in either HPLM^{dFBS} or RPMI^{dFBS}, we restricted our subsequent analyses to these early timeframes. We would speculate that culturing T lymphocytes in physiologic medium for longer time frames would have major impacts on the proliferation, activation, and metabolic state of the T cells. Similarly, metabolic status has been shown to have an impact on T cell differentiation and type of effector cytokines being secreted (Buck et al., 2015). It is likely that culture in HPLM would impact these processes as well; however, it was outside the purview of our study.

We also found that HPLM^{dFBS} had a large relative impact on the transcriptional response of activated human T cells, revealing major differences that led to our subsequent focus on extracellular [Ca²⁺]. However, many of the most significant differentially regulated genes in our dataset were associated with metabolic pathways. In particular, we found that HPLM^{dFBS} induced large increases in the expression of genes

involved in several amino acid metabolism pathways, including significant upregulation of genes that encode various rate-limiting enzymes in such pathways (*ASS1*, *PHGDH*, *PYCR1*, *GOT1*). It is likely that such differences result from marked differences in the availability of several amino acids between HPLM^{dFBS} and RPMI^{dFBS}. For instance, arginine, which is present at nearly 10-fold greater levels in basal RPMI compared with human blood and (HPLM), have been suggested to be critical for T cell proliferation, differentiation, and survival, and previous studies have described improved T cell survival upon arginine supplementation to 3 mM (Rodriguez et al., 2007; Geiger et al., 2016). Thus, it is likely that in the *in vivo* environment arginine is even more limiting than previously thought.

Our data broadly highlight the fact that commonly used conditions used to culture and examine T lymphocytes *in vitro* may not be ideal for metabolic studies, and we also specifically identify one extracellular component (calcium) that can be easily considered by others in the field. Our approach also further demonstrates the value of using HPLM to improve the modeling capacity of *in vitro* cell culture systems.

Limitations of the Study

In this work we characterize for the first time the impact of physiologic media on the metabolism and activation of human T cell *in vitro* culture and highlight the drawbacks of conventional media formulations. Although we did observe significant transcriptional changes in multiple critical metabolic pathways, we did not explore the mechanisms behind this nor the downstream impacts on longevity, memory/effector differentiation or differentiation to different subsets such as Th1, Th2, Tregs, and others. It is known that the metabolic state has a critical impact on these processes (van der Windt and Pearce, 2012; Berod et al., 2014; Lochner et al., 2015), and it is likely that physiologic media is a superior model of the *in vivo* condition; however this hypothesis remains to be tested. In addition to this, our analysis was restricted to the transcriptome and effector/proliferative functions of T lymphocytes rather than direct investigation of the metabolic state of primary cells cultured in HPLM relative to conventional media. Lastly, although we focused exclusively on T lymphocytes, it is likely that B cells, myeloid cells, and other lineages are likely to be similarly affected, although again this remains to be tested.

METHODS

All methods can be found in the accompanying [Transparent Methods supplemental file](#).

DATA AND CODE AVAILABILITY

The RNA-Seq data from this study were uploaded to GEO and may be accessed at: <https://www.ncbi.nlm.nih.gov/geo/query/acc.cgi?acc=GSE135936>.

SUPPLEMENTAL INFORMATION

Supplemental Information can be found online at <https://doi.org/10.1016/j.isci.2019.100759>.

ACKNOWLEDGMENTS

M.L.G. was a student in the NIH-University of Pennsylvania graduate partnership program and the authors would like to acknowledge the mentorship and guidance provided. We thank Ann Park, Xijin Xu, other members of the Molecular Development of the Immune System Section at the NIH, John Wherry, Sara Cherry, Pamela Schwartzberg, and Igor Brodsky for helpful discussions as well as technical guidance. We are grateful for financial support from the Lupus Foundation of America and Merck, Inc. The authors would also like to thank the Clinical Cancer Research Sequencing Facility for assistance in performing the RNA-Sequencing experiments and subsequent analysis, in particular; Justin Lack, Jyoti Shetty, and Bao Tran. The authors would like to thank Ryan Kissinger for assistance in creating the graphical abstract. Lastly, the authors thank Tori Yamamoto for the kind gift of the CAR-T cell lentivirus. J.R.C. is supported in part by the NIH/NCI (K22CA225864). This research was supported in part by the Intramural Research Program of the NIH, National Institute of Allergy and Infectious Diseases.

AUTHOR CONTRIBUTIONS

M.L.G., H.C.S., and M.J.L. initiated the project and designed the research. M.L.G. performed the experiments and analyzed the data with input from J.R.C., H.C.S., and M.J.L. J.R.C. prepared the HPLM media. A.B. performed bioinformatic analysis. M.L.G., H.C.S., J.R.C., and M.L. wrote the manuscript and all authors edited.

DECLARATION OF INTERESTS

The authors declare no competing interests.

Received: August 20, 2019

Revised: September 30, 2019

Accepted: December 5, 2019

Published: January 24, 2020

REFERENCES

- Berod, L., Friedrich, C., Nandan, A., Freitag, J., Hagemann, S., Harmrolfs, K., Sandouk, A., Hesse, C., Castro, C.N., Bähre, H., et al. (2014). De novo fatty acid synthesis controls the fate between regulatory T and T helper 17 cells. *Nat. Med.* **20**, 1327–1333.
- Bertin, S., Aoki-Nonaka, Y., de Jong, P.R., Nohara, L.L., Xu, H., Stanwood, S.R., Srikanth, S., Lee, J., and To, K. (2014). The ion channel TRPV1 regulates the activation and proinflammatory properties of CD4⁺ T cells. *Nat. Immunol.* **15**, 1055–1063.
- Buck, M.D., Sowell, R.T., Kaech, S.M., and Pearce, E.L. (2017). Metabolic instruction of immunity. *Cell* **169**, 570–586.
- Buck, M.D., O'Sullivan, D., and Pearce, E.L. (2015). T cell metabolism drives immunity. *J. Exp. Med.* **212**, 1345–1360.
- Cantor, J.R., Abu-Remaileh, M., Kanarek, N., Freinkman, E., Gao, X., Louissaint, A., Jr., Lewis, C.A., and Sabatini, D.M. (2017). Physiologic medium rewires cellular metabolism and reveals uric acid as an endogenous inhibitor of UMP synthase. *Cell* **169**, 258–272.e17.
- Crabtree, G.R. (1989). Contingent genetic regulatory events in T lymphocyte activation. *Science* **243**, 355–361.
- Derler, I., Jardin, I., and Romanin, C. (2016). Molecular mechanisms of STIM/Orai communication. *Am. J. Physiol. Cell Physiol.* **310**, C643–C662.
- Eagle, H. (1955). The specific amino acid requirements of a mammalian cell (Strain L) in tissue culture. *J. Biol. Chem.* **214**, 839–852.
- Favaro, E., Bensaad, K., Chong, M.G., Tennant, D.A., Ferguson, D.J., Snell, C., Steers, G., Turley, H., Li, J.L., Günther, U.L., et al. (2012). Glucose utilization via glycogen phosphorylase sustains proliferation and prevents premature senescence in cancer cells. *Cell Metab.* **16**, 751–764.
- Feske, S., Gwack, Y., Prakriya, M., Srikanth, S., Puppel, S.H., Tanasa, B., Hogan, P.G., Lewis, R.S., Daly, M., and Rao, A. (2006). A mutation in Orai1 causes immune deficiency by abrogating CRAC channel function. *Nature* **441**, 179–185.
- Geiger, R., Rieckmann, J.C., Wolf, T., Basso, C., Feng, Y., Fuhrer, T., Kogadeeva, M., Picotti, P., Meissner, F., Mann, M., et al. (2016). L-arginine modulates T cell metabolism and enhances survival and anti-tumor activity. *Cell* **167**, 829–842.e13.
- Goldstein, D.A. (1990). Serum calcium. In *Clinical Methods: The History, Physical, and Laboratory Examinations*, Third Edition, H. Walker, W. Hall, and J. Hurst, eds. (Butterworths), pp. 677–679.
- Gwack, Y., Srikanth, S., Oh-Hora, M., Hogan, P.G., Lamperti, E.D., Yamashita, M., Gelinias, C., Neems, D.S., Sasaki, Y., Feske, S., et al. (2008). Hair loss and defective T- and B-cell function in mice lacking Orai1. *Mol. Cell Biol.* **28**, 5209–5222.
- Jacobs, S.R., Herman, C.E., Maciver, N.J., Wofford, J.A., Wieman, H.L., Hammen, J.J., and Rathmell, J.C. (2018). Glucose uptake is limiting in T cell activation and requires CD28-Mediated Akt-Dependent and independent pathways. *J. Immunol.* **180**, 4476–4486.
- Kanehisa, M., Sato, Y., Furumichi, M., Morishima, K., and Tanabe, M. (2019). New approach for understanding genome variations in KEGG. *Nucleic Acids Res.* **47**, D590–D595.
- Kanehisa, M., and Goto, S. (2000). KEGG: kyoto encyclopedia of genes and genomes. *Nucleic Acids Res.* **28**, 27–30.
- Lochner, M., Berod, L., and Sparwasser, T. (2015). Fatty acid metabolism in the regulation of T cell function. *Trends Immunol.* **36**, 81–91.
- Ma, E.H., Bantug, G., Griss, T., Condotta, S., Johnson, R.M., Samborska, B., Mainolfi, N., Suri, V., Guak, H., Balmer, M.L., et al. (2017). Serine is an essential metabolite for effector T cell expansion. *Cell Metab.* **25**, 345–357.
- McCoy, T.A., Maxwell, M., and Kruse, P.F. (1959). The amino acid requirements of the jensen sarcoma in vitro. *Cancer Res.* **19**, 591–595.
- Moore, G.E., Ito, E., Ulrich, K., and Sandberg, A.A. (1966). Culture of human leukemia cells. *Cancer* **19**, 713–723.
- Moore, G., Gerner, R., and Franklin, H.A. (1967). Culture of normal human leukocytes. *JAMA* **199**, 519–524.
- Newick, K., et al. (2018). CAR T-cell therapy for solid tumors? *Cancer Discov.* **8**, 1341.
- O'Sullivan, D., van der Windt, G.J., Huang, S.C., Curtis, J.D., Chang, C.H., Buck, M.D., Qiu, J., Smith, A.M., Lam, W.Y., DiPlato, L.M., et al. (2014). Memory CD8⁺ T cells use cell-intrinsic lipolysis to support the metabolic programming necessary for development. *Immunity* **41**, 75–88.
- Pan, M., Reid, M.A., Lowman, X.H., Kulkarni, R.P., Tran, T.Q., Liu, X., Yang, Y., Hernandez-Davies, J.E., Rosales, K.K., Li, H., et al. (2016). Regional glutamine deficiency in tumours promotes dedifferentiation through inhibition of histone demethylation. *Nat. Cell Biol.* **18**, 1090–1101.
- Pearce, E.L., Walsh, M.C., Cejas, P.J., Harms, G.M., Shen, H., Wang, L.S., Jones, R.G., and Choi, Y. (2009). Enhancing CD8 T-cell memory by modulating fatty acid metabolism. *Nature* **460**, 103–107.
- Prakriya, M., Feske, S., Gwack, Y., Srikanth, S., Rao, A., and Hogan, P.G. (2006). Orai1 is an essential pore subunit of the CRAC channel. *Nature* **443**, 230–233.
- Rodriguez, P.C., Quiceno, D.G., and Ochoa, A.C. (2007). L-arginine availability regulates T-lymphocyte cell-cycle progression. *Blood* **109**, 1568–1574.
- Schug, Z.T., Peck, B., Jones, D.T., Zhang, Q., Grosskurth, S., Alam, I.S., Goodwin, L.M., Smethurst, E., Mason, S., Blyth, K., et al. (2015). Acetyl-CoA synthetase 2 promotes acetate utilization and maintains cancer cell growth under metabolic stress. *Cancer Cell* **27**, 57–71.
- Sinclair, L.V., Rolf, J., Emslie, E., Shi, Y.B., Taylor, P.M., and Cantrell, D.A. (2013). Control of amino-acid transport by antigen receptors coordinates the metabolic reprogramming essential for T cell differentiation. *Nat. Immunol.* **14**, 500–508.
- Smith-garvin, J.E., Koretzky, G.A., and Jordan, M.S. (2010). T cell activation. *Immunology* **27**, 591–619.
- Vande Voorde, J., Ackermann, T., Pfetzer, N., Sumpton, D., Mackay, G., Kalna, G., Nixon, C., Blyth, K., Gottlieb, E., and Tardito, S. (2019). Improving the metabolic fidelity of cancer models with a physiological cell culture medium. *Sci. Adv.* **5**, eaau7314.
- Werner, A., Koschke, M., Leuchtner, N., Luckner-Minden, C., Habermeier, A., Rupp, J., Heinrich, C., Conradi, R., Closs, E.I., and Munder, M. (2017). Reconstitution of T cell proliferation under arginine limitation: activated human T cells take up citrulline via L-type amino acid transporter 1 and use it to regenerate arginine after induction of argininosuccinate synthase expression. *Front. Immunol.* **8**, 864.
- van der Windt, G.J.W., and Pearce, E.L. (2012). Metabolic switching and fuel choice during T-cell differentiation and memory development. *Immunol. Rev.* **249**, 27–42.
- Zhang, S.L., Yu, Y., Roos, J., Kozak, J.A., Deerinck, T.J., Ellisman, M.H., Stauderman, K.A., and Cahalan, M.D. (2005). STIM1 is a Ca²⁺ sensor that activates CRAC channels and migrates from the Ca²⁺ store to the plasma membrane. *Nature* **437**, 902–905.
- Zimmermann, J., Radbruch, A., and Chang, H.D. (2015). A Ca²⁺ concentration of 1.5 mM, as present in IMDM but not in RPMI, is critical for maximal response of Th cells to PMA/ionomycin. *Eur. J. Immunol.* **45**, 1270–1273.

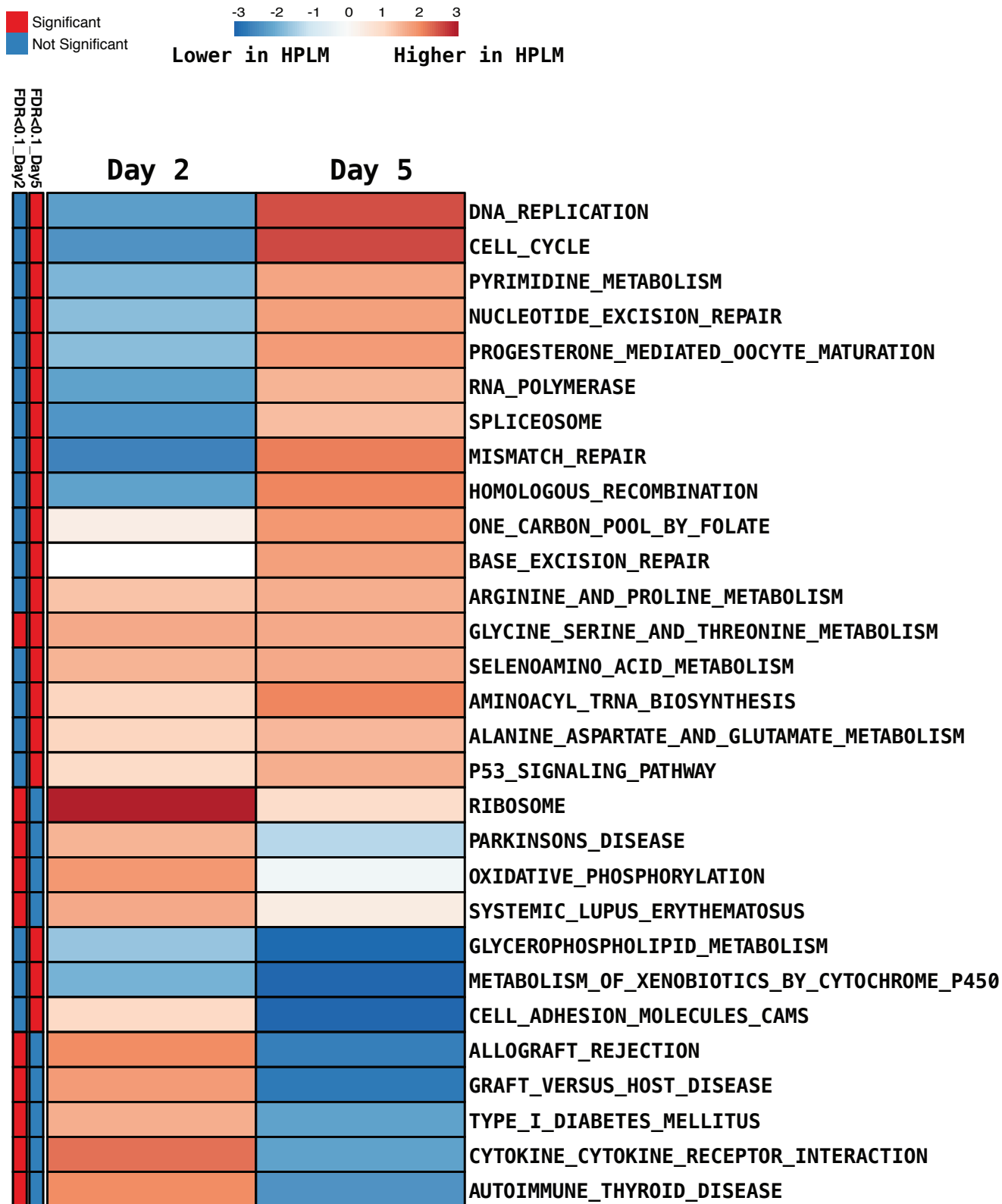
ISCI, Volume 23

Supplemental Information

Human Plasma-like Medium

Improves T Lymphocyte Activation

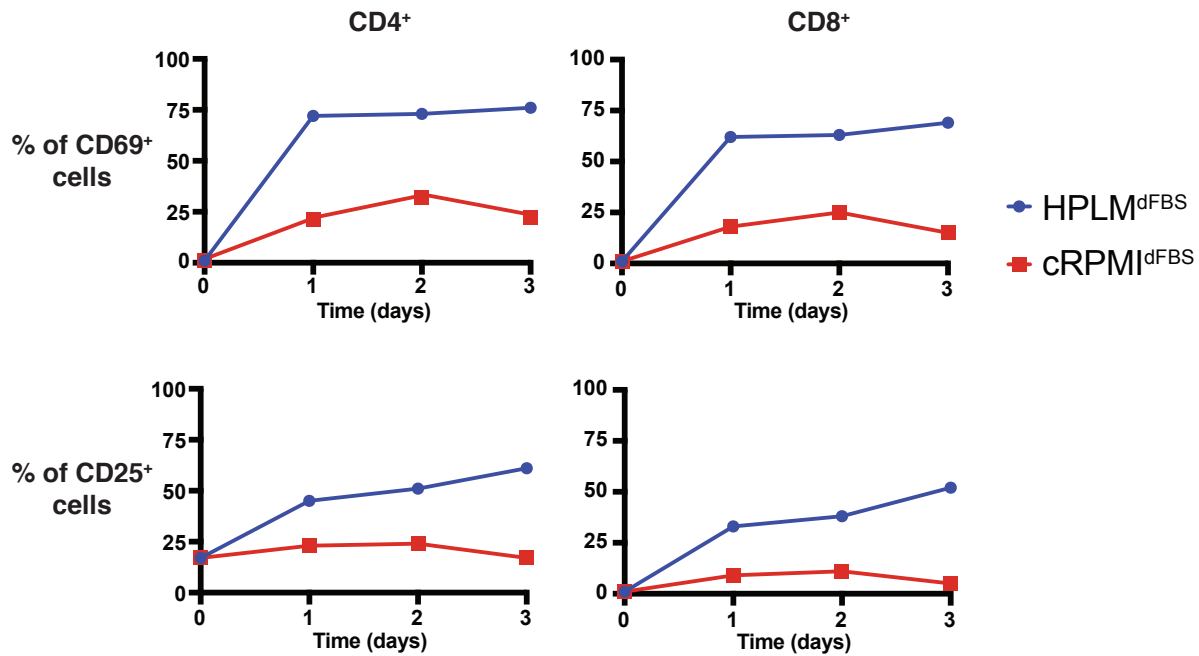
Michael A. Leney-Greene, Arun K. Boddapati, Helen C. Su, Jason R. Cantor, and Michael J. Lenardo



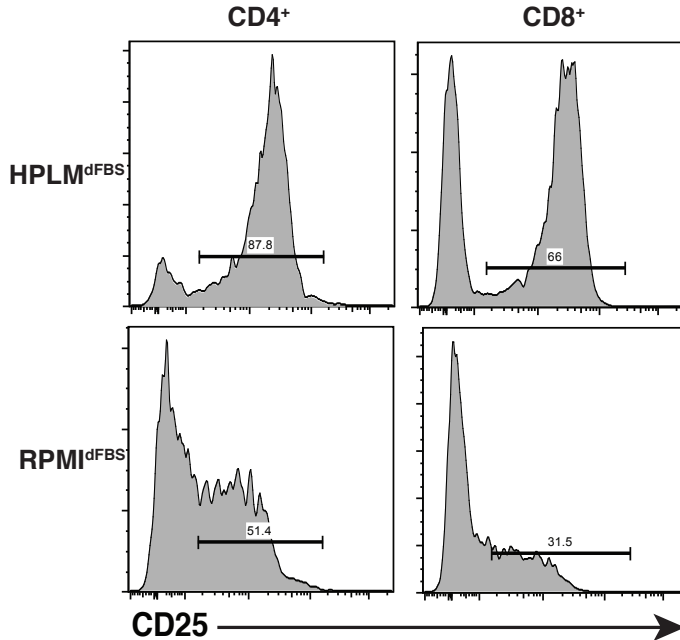
Supplemental Figure 1 – GSEA of purified naïve human T cells activated in either HPLM^{dFBS} or RPMI^{dFBS}, related to Figure 1C-D.

Plot showing KEGG pathways enriched at either 48 or 120 hours following stimulation in either HPLM^{dFBS} or RPMI^{dFBS}.

A Human pan naive T cells



B Murine T cells



Supplemental Figure 2 – Activation kinetics of murine/human T cells cultured in HPLM^{dFBS} or RPMI^{dFBS}. Data related to Figure 2A.

- (A) Daily quantification of CD25 and CD69 of pan human naive T cells cultured in either HPLM^{dFBS} or RPMI^{dFBS}. Data shown are a single experiment representative of 4 repeats.
- (B) Quantification of CD25 and CD69 24 hours post-activation of splenic murine T cells cultured in either HPLM^{dFBS} or RPMI^{dFBS}. Data is representative of two experiments.

Supplemental Table 1: Detailed Media Composition, Related to Figure 1

	Concentration (μM)		
	RPMI	HPLM-MIN	HPLM
Glucose	11111	5000	5000
<i>Proteinogenic Amino acids</i>			
Alanine	0	430	430
Arginine	1149	110	110
Asparagine	378	50	50
Aspartate	150	20	20
Cysteine	0	40	40
Cystine	208	100	100
Glutamate	136	80	80
Glutamine	2055	550	550
Glycine	133	300	300
Histidine	97	110	110
Hydroxyproline	153	0	0
Isoleucine	382	70	70
Leucine	382	160	160
Lysine	219	200	200
Methionine	101	30	30
Phenylalanine	91	80	80
Proline	174	200	200
Serine	286	150	150
Threonine	168	140	140
Tryptophan	25	60	60
Tyrosine	11	80	80
Valine	171	220	220
<i>Ions</i>			
Na⁺	138525	132271	132271
K⁺	5333	4142	4142
Ca²⁺	424	2390	2390
Mg²⁺	407	830	830
NH⁴⁺	0	40	40
Cl⁻	108781	116196	116196
HCO³⁻	23809	24000	24000
PO₄³⁻	5634	966	966
SO₄²⁻	407	350	350
NO³⁻	848	80	80

Additional Polar Metabolites

2-hydroxybutyrate		50
3-hydroxybutyrate		50
4-hydroxyproline		20
Acetate		40
Acetone		60
Acetylcarnitine		5
Acetylglycine		90
α-aminobutyrate		20
α-ketoglutarate		5
Betaine		70
Carnitine		40
Citrate		130
Citrulline		40
Creatine		40
Creatinine		75
Formate		50
Fructose		40
Galactose		60
Glutathione		25
Glycerol		120
Hypoxanthine		10
Lactate		1600
Malate		5
Malonate		10
Ornithine		70
Pyruvate		50
Succinate		20
Taurine		90
Urea		5000
Uric Acid		350
Uridine		3

MATERIALS AND METHODS

Study Subjects

Anonymized blood samples were received from the NIH Department of Laboratory Medicine and processed in order to isolate PBMCs.

Cell Culture

In order to maintain consistency and reduce potential batch effects RPMI was prepared from powder (US Biologicals). Fresh L-glutamine (Gibco) and dialyzed FBS (Thermo Fisher Scientific) were added immediately prior to use at a final concentration of 2 mM and 10% by volume respectively. HPLM^{dFBS} was prepared as previously described (Cantor *et al.*, 2017) along with four additional compounds: Uridine (3 μ M), α -ketoglutarate (5 μ M), acetylcarnitine (5 μ M) and malate (5 μ M). HPLM^{dFBS}-Min was prepared as HPLM^{dFBS} but lacking all defined components other than glucose, proteinogenic amino acids, vitamins, salts, and dialyzed serum. (see Supplemental Table 1). RPMI was supplemented with 10% of either dialyzed (RPMI^{dFBS}) or unmodified FBS (RPMI^{FBS}). For long-term T cell proliferation assays, human recombinant IL-2 (Roche) was also added fresh immediately prior to use at a final concentration of 100 IU/ml. X-VIVO 15 media (Lonza) was used without additional serum. AIM-V media was a mixture of 50% RPMI and 50% AIM-V (Gibco) supplemented with 5% Normal Human Serum (Valley Biomedical). RPMI-Metabolites was prepared by supplementing RPMI with both 10% dialyzed FBS and 31 additional polar metabolites at concentrations defined in basal HPLM.

Flow Cytometry

For simple surface stains, cells were washed once in phosphate buffered saline (PBS) and stained with 50 μ l of Zombie AquaTM viability (Biolegend) dye for 20 minutes on ice. After washing once with FACS buffer (PBS containing 5% FBS and 0.1% NaN₃), cells were stained in 50 μ l of FACS buffer containing diluted antibodies for 30 minutes on ice. Cells were then washed three times in FACS buffer and fixed before acquisition on either a LSRII or LSRFortessa (BD Biosciences). For intracellular cytokine staining following restimulation, cells were washed with PBS, stained in antibodies in 50 μ l of FACS buffer for 30 minutes on ice. Cells were then washed three times in FACS buffer, then incubated for 20 minutes in 50 μ l of Fixation/Permeabilization solution (BD Biolegend). Cells were washed three times in Perm/Wash buffer (BD Biolegend), then stained for 30 minutes on ice in antibodies diluted in

Perm/Wash buffer. Cells were washed three times, then resuspended in Perm/Wash buffer and acquired on an LSRII. Data was analyzed using FlowJo v. 9.9.5.

T cell Activation and expansion Analysis

Peripheral blood mononuclear cells were freshly isolated from blood from healthy human donors of both sexes ranging from 25-60 years old. Naïve T cells were enriched via a negative selection kit (Miltenyi Biotech, 130-097-095) and either used immediately or stored in liquid nitrogen in a 9:1 mixture of FBS: dimethyl sulfoxide. For short-term activation assays, 96 well Nunc Maxisorp plates were coated with 1 to 10 ug/ml of anti-CD3/anti-CD28 antibodies in PBS for 2 to 4 hours at 37°C. Plates were then washed twice with PBS and enriched naïve T cells were added in the indicated media formulations. Levels of activation markers were measured by flow cytometry 16 to 24 hours later. For proliferation assays, cells were stained with Celltrace Violet and then activated as above. After three days, cells were transferred to a new plate with fresh media and analyzed by flow cytometry after another two days. Alternatively, for murine T cells, crude splenic cells were isolated and cultured on plate-bound anti-CD3/CD28 antibodies (clones 2C11 and clone 37.51 respectively, Biolegend). One day later cells were analyzed by flow cytometry as described above to measure levels of activation markers.

Calcium flux measurements

Purified naïve human T cells were cultured in RPMI for 16 to 24 hours following isolation or thawing from liquid nitrogen storage. Cells were then loaded with Indo-1 calcium Indicator dye (Thermo Fisher Scientific) resuspended in PowerLoad™ (Thermo Fisher Scientific) at a concentration for 20 minutes at room temperature. and stained for surface markers. Anti-CD3 (Hit3 α) was added at 10 ug/ml, samples were acquired for 20 seconds to determine background levels, then F(ab')₂ fragments (Jackson ImmunoResearch) were added at 13 ug/ml in order to crosslink the TCR. The flux was then recorded for another 130-180 seconds and analyzed by measuring the ratio of fluorescence in the two channels.

T cell cytokine production assays

Human T lymphocytes were activated and expanded in IL-2-containing media as described above for 15 to 20 days. The night before the assay, cells were placed in fresh media (either HPLM^{dFBS} or RPMI^{dFBS}) containing IL-2, and the following day were restimulated with either 1 μ g/ml each of anti-CD3 (HIT3 α , Biolegend) or PMA and ionomycin (Biolegend) for 6 or 5 hours respectively. Four hours prior to analysis, Brefeldin A was added (Biolegend). Following the

restimulation, cells were washed in PBS, placed on ice and stained according to the protocol described above.

Retroviral Transductions

CD19-CAR expressing retrovirus was produced as previously described (Kerkar *et al.*, 2011). 96-well plates were coated with Retronectin (Clontech) overnight at 4°C, washed and blocked with 2.5% bovine serum albumin (BSA), washed again and then bound to retrovirus by centrifuging the plates with viral supernatant for two hours at 37°C. The supernatants were then aspirated and human T lymphocytes that had been activated the previous day were added to the plate in the medium indicated. 48 hours following transduction, the cells were stained with Biotin-Protein L (Genscript) followed by fluorescently-conjugated streptavidin.

RNA-Sequencing

RNA was isolated from cells using trizol (Thermo Fisher). We then used 0.1 – 1 ug of total RNA as input for mRNA capture with oligo-dT coated magnetic beads using the Illumina TruSeq protocol. The mRNA was fragmented, and then a random-primed cDNA synthesis was performed. The resulting double-strand cDNA was used as the input for a standard Illumina library prep with end-repair, adapter ligation and PCR amplification and then quantitated by qPCR followed by cluster generation and sequencing. RNA-Seq processing was conducted using the Pipeliner RNA-Seq workflow for quality assessment. For gene expression analysis, reads were trimmed to remove adapters and low-quality regions using Trimmomatic v0.33 (Bolger, Lohse and Usadel, 2014). Trimmed reads were aligned to the human GRCh38 reference genome and Gencode release 28 annotation using STAR v2.5.3 run in 2-pass mode (Dobin *et al.*, 2013). MultiQC v1.1 was used to aggregate QC metrics from picard, FastQC v0.11.5, FastQ screen v0.9.3 and RseQC to assess read and alignment quality (Wang, Wang and Li, 2012; Ewels *et al.*, 2016; Brown, Pirrung and Mccue, 2017; Wingett and Andrews, 2018). RSEM v1.3.0 was used for gene-level quantification and the resultant raw counts were voom-quantile normalized and batch corrected using the R package limma v3.38.3. Only genes that passed a 1 CPM threshold across a minimum of 3 samples based on the size of the smallest library were carried forward for differential expression testing. Pre-ranked gene set enrichment analysis (GSEA) was carried out using Gene Set Enrichment Analysis tool (GSEA v3.0) and Kegg pathways from MSigDB (Liberzon *et al.*, 2011). Heatmap figures for visualization of gene

expression and normalized enrichment score (NES) were generated using the heatmap.2 function from the R package gplots v3.0.1.1 and Clustvis respectively (Metsalu and Vilo, 2015).

Quantification and Statistical Analyses

One-way ANOVA with Dunnett's/Tukey's multiple comparisons test and Student's t test were performed using Prism software (GraphPad). Descriptions of sample size and particular tests used can be found in the figure legends.

Supplemental References

Bolger, A. M., Lohse, M. and Usadel, B. (2014) 'Trimmomatic: A flexible trimmer for Illumina sequence data', *Bioinformatics*, 30(15), pp. 2114–2120. doi: 10.1093/bioinformatics/btu170.

Brown, J., Pirrung, M. and Mccue, L. A. (2017) 'FQC Dashboard: Integrates FastQC results into a web-based, interactive, and extensible FASTQ quality control tool', *Bioinformatics*, 33(19), pp. 3137–3139. doi: 10.1093/bioinformatics/btx373.

Cantor, J. R. *et al.* (2017) 'Physiologic Medium Rewires Cellular Metabolism and Reveals Uric Acid as an Endogenous Inhibitor of UMP Synthase', *Cell*. Elsevier, 169(2), pp. 258-272.e17. doi: 10.1016/j.cell.2017.03.023.

Dobin, A. *et al.* (2013) 'STAR: Ultrafast universal RNA-seq aligner', *Bioinformatics*, 29(1), pp. 15–21. doi: 10.1093/bioinformatics/bts635.

Ewels, P. *et al.* (2016) 'MultiQC: Summarize analysis results for multiple tools and samples in a single report', *Bioinformatics*, 32(19), pp. 3047–3048. doi: 10.1093/bioinformatics/btw354.

Kerkar, S. P. *et al.* (2011) 'Genetic engineering of murine CD8+ and CD4+ T cells for pre-clinical adoptive immunotherapy studies', *J. Immunother.*, 34(4), pp. 343–352. doi: 10.1097/CJI.0b013e3182187600.Genetic.

Liberzon, A. *et al.* (2011) 'Molecular signatures database (MSigDB) 3.0', *Bioinformatics*, 27(12), pp. 1739–1740. doi: 10.1093/bioinformatics/btr260.

Metsalu, T. and Vilo, J. (2015) 'ClustVis: A web tool for visualizing clustering of multivariate data using Principal Component Analysis and heatmap', *Nucleic Acids Research*, 43(W1), pp. W566–W570. doi: 10.1093/nar/gkv468.

Wang, L., Wang, S. and Li, W. (2012) 'RSeQC: Quality control of RNA-seq experiments', *Bioinformatics*, 28(16), pp. 2184–2185. doi: 10.1093/bioinformatics/bts356.

Wingett, S. W. and Andrews, S. (2018) 'FastQ Screen: A tool for multi-genome mapping and quality control', *F1000Research*, 7(May), p. 1338. doi: 10.12688/f1000research.15931.2.